Available online at www.sciencedirect.com

SciVerse ScienceDirect

Ceramics International 39 (2013) 2165–2170

CERAMICS INTERNATIONAL

www.elsevier.com/locate/ceramint

Short communication

Microwave assisted sol–gel synthesis of chlorine doped lithium vanadium phosphate

Jinhan Yao[a,*], Zhitao Jia[a], Pinjie Zhang[a], Chaoqi Shen[a], Jianbo Wang[a], Kondo-Francois Aguey-Zinsou[b], Chun'an Ma[a], Lianbang Wang[a,*]

[a]State Key Laboratory Breeding Base of Green Chemistry-Synthesis Technology, College of Chemical Engineering and Material Science, Zhejiang University of Technology, Hangzhou, Zhejiang PR China

[b]School of Chemical Engineering, The University of New South Wales, Sydney, Australia

Received 28 July 2012; received in revised form 30 July 2012; accepted 30 July 2012
Available online 7 August 2012

Abstract

A microwave assisted sol–gel method was adapted to synthesize Cl-doped $Li_3V_2(PO_4)_3$/C powder. The structural, morphological and electrochemical properties were characterized by X-ray diffraction, scanning and transmission electron microscopy, Raman scattering spectroscopy, and galvanostatic charge–discharge cycling. Experimental results further show that fine Cl-doped $Li_3V_2(PO_4)_3$/C powder can be synthesized within 20 min under microwave heating and the Cl-doping process contributes to induce the lattice distortion, modify the particle morphology, and increase the electronic conductivity. The Cl-doped $Li_3V_2(PO_4)_3$/C electrode presents a high initial discharge capacity of 125.1, 117.2, 110.5, 101.4, 90.7 and 72.3 mAh g^{-1} at 0.1, 0.5, 1, 2, 5 and 10C between 3.0 and 4.3 V, respectively. The improvement can be ascribed to the enhanced electronic conductivity and electrode kinetics due to the micro-structural modification promoted by Cl-doping.

Keywords: B. Composites; Microwave; Sol–gel chemistry

1. Introduction

The enhancement of synthesis technique is of great importance in improving the electrochemical performance of oxides or polyanion oxides used in energy storage and conversion applications [1–5]. In particular, finding a convenient and energy efficient synthetic route has become increasingly urgent with the rapid development in this area. In recent years, as part of efforts for identifying new cathode material for rechargeable lithium batteries, lithium vanadium phosphate ($Li_3V_2(PO_4)_3$, LVP) is regarded as a promising cathode material proposed for lithium ion batteries due to its large capacity and high discharge potential [6–14]. However, $Li_3V_2(PO_4)_3$ has a low intrinsic electrical conductivity, and thus the morphology and composition modifications were used and proved to be effective in altering the electrochemical properties, such as particle size reduction, carbon coating and (cation) doping etc. [15–23]. Indeed, all these modification strategies were closely correlated to the synthetic method. In this regard, sol–gel methods are advantageous over the solid-state reaction in preparation of LVP, as the starting materials (usually containing several types of raw substance for polyanion materials) can be mixed in the molecular level, which leads to a very high degree of homogeneity [13, 15–17, 20–22]. However, sol–gel method, with the process complexity, still requires long time sintering of the gel in the final stage in order to obtain the final product, and therefore increases the reaction time inevitably. In this regard, microwave synthesis is a powerful technique for the synthesis of ceramics in a remarkably short time under microwave radiation [24,25]. During the synthesis, since the microwave energy is absorbed directly by the bulk precursor mixture, uniform and rapid heating can be achieved within several minutes. Therefore, utilizing microwave energy for the thermal treatment could lead to a very fine particle because

*Corresponding author. Tel.: +86 571 88320611; fax: +86 571 88320832.
E-mail addresses: jhyao@zjut.edu.cn (J. Yao), wanglb99@zjut.edu.cn (L. Wang).

0272-8842/$ - see front matter © 2012 Elsevier Ltd and Techna Group S.r.l. All rights reserved.
http://dx.doi.org/10.1016/j.ceramint.2012.07.100

of the shorter reaction time and highly concentrated local heating.

Previously, Liu et al. [26] proposed a Cl doped spinel $Li_{1.06}Mn_2O_{3.94}Cl_{0.06}$ cathode material. This material exhibited better cycling ability at ambient and elevated temperatures (55 °C) compared to the un-doped counterpart, due to a highly reversible spinel structure resulting from the chlorine doping. Therefore, it can be found that chlorine doping is also an effective method to optimize the properties of electrode materials.

In this work, we for the first time, adopted a microwave-assisted sol–gel method to prepare a Cl-doped $Li_3V_2(PO_4)_3$/C powder, and the effect of Cl doping on the electrochemical properties of $Li_3V_2(PO_4)_3$/C were investigated in detail. Carbon coating was used to ensure the electronic conductivity on the surface of $Li_3V_2(PO_4)_3$ particles, and the citric acid was the carbon source. The undoped sample and Cl-doped sample were synthesized through the same procedure for comparison except for the usage of Cl source.

2. Experimental

2.1. Microwave-assisted synthesis of Cl-doped $Li_3V_2(PO_4)_3$/C

The Cl-doped $Li_3V_2(PO_4)_3$/C compounds were prepared by a microwave assisted sol–gel method employing $CH_3COO\text{-}Li \cdot 2H_2O$, NH_4VO_3, $NH_4H_2PO_4$ and NH_4Cl as raw materials in the molar ratio of 3.1:2:2.9:0.1. Citric acid was used here not only as a chelating reagent but also as a source of carbon to coat the materials with carbon layer. The mol ratio citric acid: vanadium = 2:1 was selected. An over-dosed usage of Li salt is to compensate any Li loss during the high temperature synthesis [27]. A typical synthetic procedure consisted of first dissolving citric acid and NH_4VO_3 in deionized water with magnetic stirring at 80 °C. After a clear blue solution formed, a mixture of $CH_3COOLi \cdot 2H_2O$, $NH_4H_2PO_4$ and NH_4Cl was added to the solution while stirring for 5 h. After evaporating the water at 80 °C, the blue solution became a gel. The resulting gel was put into a vacuum drying oven at 120 °C for 10 h to eliminate the water adequately. Finally, the resulting powder was reground and placed in a microwave oven (Makewave co., Ltd, 800 W) run at 350 W power for 20 min to yield the final LVP or Cl doped LVP products.

2.2. Characterization method

Structural and crystallographic analyses were performed by X-ray diffraction (XRD) using PANalytical X'Pert Pro with Cu Kα radiation. The diffraction data were recorded in the 2θ range of 10–60° with a step of 0.02°. The morphologies of samples were characterized by scanning electron microscope (SEM, Hitachi S-4800) and transmission electron microscope (TEM, FEI Tec-nai G2-F30). Raman scattering spectroscopy (LABRAM HR-800) was recorded at room temperature with the wave number shift from 4000 to 100 cm^{-1} in ultraviolet laser excitation line of 325 nm. The carbon content of the prepared materials was measured by a Thermo Fisher Flash EA 1112 analyzer.

Electrochemical performances of the samples were evaluated in coin-type cells. To prepare the electrodes used for the electrochemical performances measurement, the powders of pristine $Li_3V_2(PO_4)_3$/C and Cl-doped $Li_3V_2(PO_4)_3$/C were mixed with acetylene black and polyvinylidine fluoride (PVDF) binder in a weight ratio of 80:15:5 respectively in N-methyl-2-pyrrolidone (NMP) to ensure the homogeneity . The obtained slurry was uniformly pasted onto the aluminum current collectors and the electrodes were dried at 120 °C in vacuum for 12 h. Subsequently, CR2032 coin-type cells were assembled in an argon-filled glove box using a Celgard 2400 membrane as a separator and 1 M LiPF6 in EC:DMC:EMC (1:1:1 vol%) as the electrolyte. A lithium foil was used as the counter and reference electrodes. The coin cells were galvanostatically charged and discharged over a voltage range of 3.0–4.3 V (vs. Li/Li^+) at room temperature on a Land (Wuhan, China) battery tester. Cyclic voltammetry (CV) was measured by an electrochemical working station (PARSTAT 2273, Princeton Applied Research, US) at a scan rate of 0.5 mV s^{-1} between 3.0 and 4.3 V.

3. Results and discussion

The Rietveld refinement of Cl-doped $Li_3V_2(PO_4)_3$/C was performed, and the result is shown in Fig. 1; the doped material is well crystallized in orthorhombic structure without any unexpected phase, which indicates that the microwave-assisted sol–gel method is effective in preparing the LVP materials. The structural parameters of pristine $Li_3V_2(PO_4)_3$/C and Cl-doped $Li_3V_2(PO_4)_3$/C were summarized in Table 1. *a*, *b* and *c* values of the latter are shrunken by 0.24%, 0.19% and 0.15%, respectively, which may be caused by Cl^- ions introduction into $Li_3V_2(PO_4)_3$ matrix.

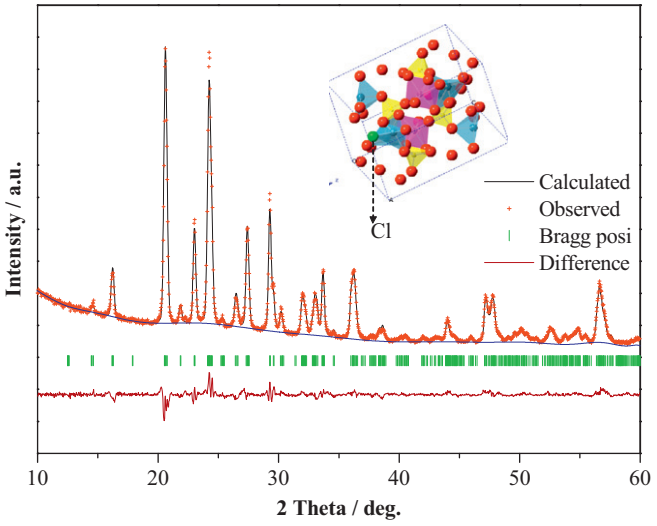

Fig. 1. Refinement result of the Cl-doped $Li_3V_2(PO_4)_3$/C sample with the observed, calculated, and difference profiles.

Table 1
Lattice constants of pristine and Cl-doped $Li_3V_2(PO_4)_3$/C.

	Lattice parameters					*R* value	
	a (Å)	*b* (Å)	*c* (Å)	*β*	*V* (Å^3)	R_{wp} (%)	R_p (%)
$Li_3V_2(PO_4)_3$/C	8.523	8.453	12.003	90.34	864.7	6.12	5.02
Cl-doped $Li_3V_2(PO_4)_3$/C	8.502	8.437	11.985	90.48	859.7	6.26	5.14

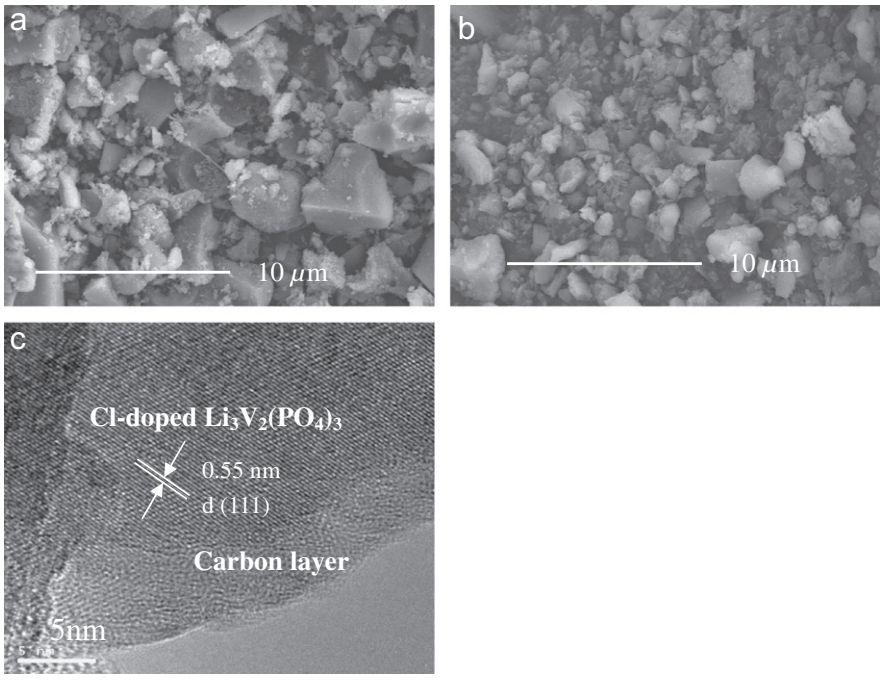

Fig. 2. SEM images of $Li_3V_2(PO_4)_3$/C (a), Cl-doped $Li_3V_2(PO_4)_3$/C (b), and TEM image of Cl-doped $Li_3V_2(PO_4)_3$/C (c).

The incorporated Cl^- tends to occupy randomly the O sites (located in P–O sub-lattice) in the crystal lattice of $Li_3V_2(PO_4)_3$.

The morphologies of pristine $Li_3V_2(PO_4)_3$/C and Cl-doped $Li_3V_2(PO_4)_3$/C were observed by SEM. Fig. 2a shows that the size of the particles of $Li_3V_2(PO_4)_3$/C ranges from one micrometer to several micrometers. For the Cl-doped $Li_3V_2(PO_4)_3$/C, well-crystallized shapes and a relatively uniform particle size distribution are observed (Fig. 2b). The reduction of particle size could be attributed to the Cl source addition which interfered with the growth of the grains. In the TEM image in Fig. 2c, the dark region is the $Li_3V_2(PO_4)_3$ particle, the inter-planar distance is 5.50 Å, which corresponds to (111) plane of $Li_3V_2(PO_4)_3$ phase. The light grey region is carbon, indicating that the $Li_3V_2(PO_4)_3$ particles are coated by conductive carbon tightly. The presence of carbon would also inhibit the crystal growth of $Li_3V_2(PO_4)_3$ during heat treatment and provide good electronic contact between $Li_3V_2(PO_4)_3$ particles. The additional carbon source as well as the resultant amount of carbon in the Cl-doped $Li_3V_2(PO_4)_3$/C composites may have a major influence on the electrochemical performance of the materials. The carbon content of two materials was ca. 3.11wt%.

As an important aid investigating the structure of the carbon, the Raman measurement was adopted, and the result was shown in Fig. 3. The Raman spectrum of the Cl-doped $Li_3V_2(PO_4)_3$/C composite was detected in the range of 1000–1800 cm^{-1}. In the spectrum, two intense broad bands at 1594.4 cm^{-1} and 1326.6 cm^{-1} are attributed to the graphite band (G-band) and the disorder-induced phonon mode (D-band), respectively. The relative intensity ratio, $R=I_D/I_G$, defines the level of order and in-plane crystal size for pyrolytic carbon, which is helpful for improving the electronic conductivity and electrochemical performance of $Li_3V_2(PO_4)_3$/C [28,29]. Therefore, it is expected that the efficient carbon-coated $Li_3V_2(PO_4)_3$ composite would exhibit favorable electrochemical properties.

The initial CV curves for pristine $Li_3V_2(PO_4)_3$/C and Cl-doped $Li_3V_2(PO_4)_3$/C are shown in Fig. 4. Both curves show a similar profile, and there are three oxidation peaks and three reduction peaks in CV curves, which indicate that the reaction behavior does not change during the

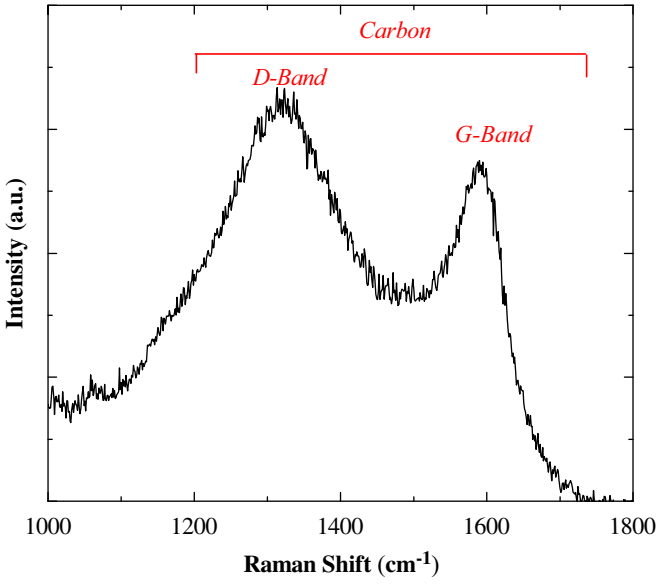

Fig. 3. Raman scattering spectrum of Cl-doped $Li_3V_2(PO_4)_3$/C.

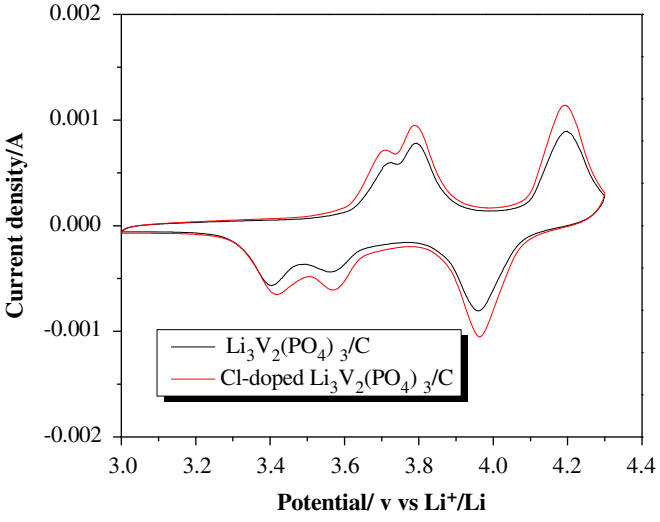

Fig. 4. CV curves of pristine $Li_3V_2(PO_4)_3$/C and Cl-doped $Li_3V_2(PO_4)_3$/C measured with a scanning rate of 0.5 mV s^{-1} between 3.0 and 4.3 V.

lithium extraction/insertion process for the coated electrode. As shown in Fig. 4, the three oxidation peaks of pristine $Li_3V_2(PO_4)_3$/C are located at about 3.72, 3.79 and 4.20 V, respectively, and the three reduction peaks are located around at 3.41, 3.56 and 3.95 V, respectively. The extraction and intercalation potentials are similar to those reported by Saidi et al. [13]. However, in the case of Cl-doped $Li_3V_2(PO_4)_3$/C electrode, the oxidation peaks shift down to 3.70, 3.78 and 4.19 V, respectively, while the reduction peaks shift up to 3.42, 3.57 and 3.97 V, respectively. In the case of $Li_3V_2(PO_4)_3$/C, the corresponding oxidation peaks shift to higher potentials, and the reduced peaks shift to lower potentials, which indicates that the $Li_3V_2(PO_4)_3$/C has the higher overpotentials for the lithium extraction/insertion process. The introduction of Cl^- into the lattice of orthorhombic structure weakened

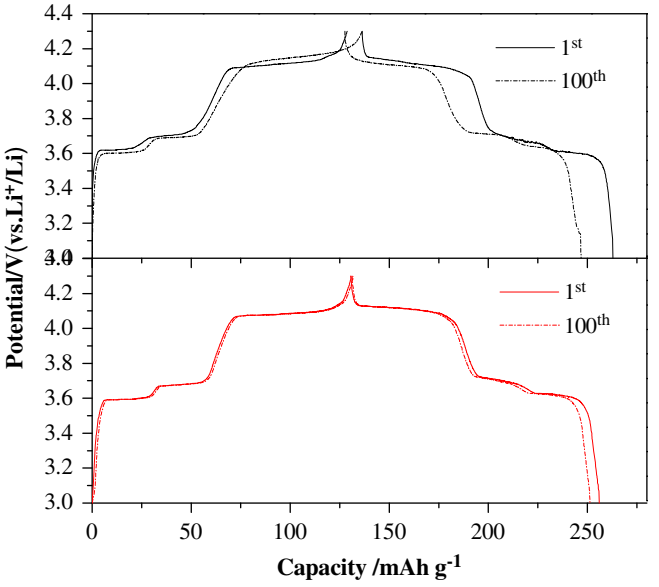

Fig. 5. The 1st and 100th charge/discharge curves of $Li_3V_2(PO_4)_3$/C (a) and Cl-doped $Li_3V_2(PO_4)_3$/C (b) in the voltage range of 3.0–4.3 V, both at 0.2c rate.

the Li–O bonding, and thus facilitated the extraction of Li ion from $Li_3V_2(PO_4)_3$/C. The results of CV tests convince us that the kinetics of electrochemical reaction of $Li_3V_2(PO_4)_3$/C is improved by Cl-doping.

The initial charge–discharge curves for $Li_3V_2(PO_4)_3$/C and Cl-doped $Li_3V_2(PO_4)_3$/C at 0.2C in the voltage range of 3.0–4.3 V are presented in Fig. 5. It can be seen that the profiles of the charge/discharge curves for the two samples are almost the same. The voltage profiles exhibit three charge plateaus around 3.59, 3.68 and 4.07 V and three corresponding discharge plateaus around 3.59, 3.65 and 4.11 V, which are identified as the two-phase transition processes during the electrochemical reaction [14,30,31]; these regions correspond to three compositional regions of $Li_{3-x}V_2(PO_4)_3$, where $x=0.0$–0.5, 0.5–1.0 and 1.0–2.0. The first lithium ion was extracted in two steps (3.59 and 3.68 V) for the mixed $V3^+/V4^+$ couple because of the existence of ordered phases at $Li_{2.5}V_2(PO_4)_3$ and $Li_2V_2(PO_4)_3$. Then, a single-step removal of the second lithium ion at 4.07 V can be observed, which corresponds to a 0.39 V step from the $V3^+/V4^+$ couple to the $V5^+/V4^+$ couple. The initial discharge capacities for pristine $Li_3V_2(PO_4)_3$/C and Cl-doped $Li_3V_2(PO_4)_3$/C are 126.3 and 127.1 mAh g^{-1}, respectively, indicating that more Li ions can be reversibly extracted. These values are close to the theoretical capacity of monoclinic $Li_3V_2(PO_4)_3$ (130 mAh g^{-1}, between 3.0 and 4.3 V vs. Li/Li^+). From the 100th charge/discharge curves, the effects of modification with Cl^- ion are apparent; the Cl-doped $Li_3V_2(PO_4)_3$/C composite yields the discharge capacity of 125.5 mAh g^{-1}, which is higher than that of the pristine $Li_3V_2(PO_4)_3$/C (118 mAh g^{-1}) composite.

To examine the effect of the Cl element addition on the electrochemical performance of the Cl-doped $Li_3V_2(PO_4)_3$/C composite, the rate capability was examined by applying different current densities to the cell (Fig. 6). The cells were

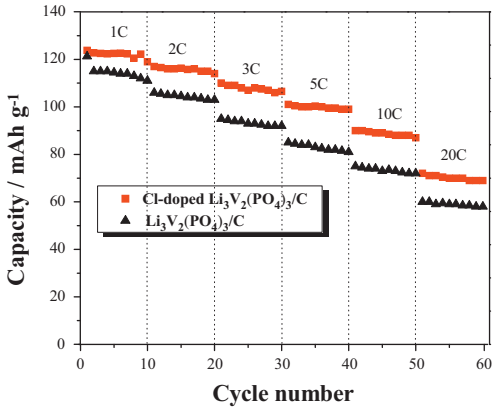

Fig. 6. Cycling performances of pristine $Li_3V_2(PO_4)_3$/C and Cl-doped $Li_3V_2(PO_4)_3$/C cathodes with different rates in the voltage range of 3.0–4.3 V.

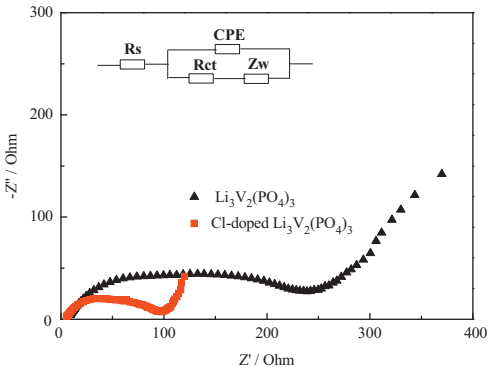

Fig. 7. EIS spectra of the $Li_3V_2(PO_4)_3$/C and Cl-doped $Li_3V_2(PO_4)_3$/C, and the inserted figure is the equivalent circuit for the Nyquist plots.

first cycled at 1C, and the rate was increased in stages to 20C in the voltage range of 3.0–4.3 V. For each sample, the discharge capacity decreases with increasing current density and the Cl-doped sample displays excellent rate performances. No obvious loss in capacity is observed over cycling at each rate. At each current density, it is obvious that the cyclability of the Cl-doped sample is better than that of pristine $Li_3V_2(PO_4)_3$/C. The initial discharge capacity for the doped sample is 121.1 mAh g^{-1} and the discharge capacity remains 85.2 mAh g^{-1} at 10C current density, but the discharge capacity of pristine $Li_3V_2(PO_4)_3$/C degrades sharply and falls from the initial 111.2 mAh g^{-1} at 1C to 70.6 mAh g^{-1} at 10C after 60 cycles. This clearly demonstrates that our Cl-doped $Li_3V_2(PO_4)_3$/C is tolerant to varied charge and discharge currents, which is a desirable characteristic required for application in high-power batteries.

To further understand the electrochemical dynamic behavior of electrodes, electrochemical impedance spectroscopy (EIS) measurements were performed on the electrodes. The typical Nyquist plots of EIS are presented in Fig. 7 for the pristine and Cl-doped $Li_3V_2(PO_4)_3$/C. Similar EIS patterns are observed for both samples. The semicircle in the high-frequency region represents charge-transfer resistance. This impedance spectra can be explained with solution resistance (R_s), a constant phase element (CPE) associated with the particle-to-particle resistance (R_{ct}), and the Warburg impedance (Z_w) which is attributed to the diffusion of Li-ions in the bulk materials [25–28]. The Cl-doped $Li_3V_2(PO_4)_3$/C sample exhibited smaller R_{ct} which means that Cl^- doping would effectively enhance the on charge transfer. This observation could mean Cl^- doping enhances the electrochemical activity of $Li_3V_2(PO_4)_3$ and facilitates the electron diffusion in the Li^+ insertion and extraction process which are both favorable for improving the cycle performance of positive lithium vanadium phosphate materials.

4. Conclusion

Cl-doped $Li_3V_2(PO_4)_3$/C and $Li_3V_2(PO_4)_3$/C were both prepared via microwave assisted sol–gel route. The relationship between the electrochemical performances and the microstructure changes was investigated through XRD, SEM, TEM and CV. The electrochemical measurements demonstrate that the Cl-doped material exhibits not only enhanced initial capacity and coulombic efficiency, but also high rate capability, indicative of a remarkably improved electrochemical performance as compared with the pristine $Li_3V_2(PO_4)_3$/C. The Cl-doped $Li_3V_2(PO_4)_3$/C sample exhibited initial discharge capacities of 121.1, 117.2, 110.5, 101.4, 85.2 and 68.5 mAh g^{-1} as it was discharged at 1, 2, 3, 5, 10 and 20C rates, respectively. Therefore, the microwave assisted sol–gel method and Cl^- doping method could be a promising approach to improve the electrochemical properties of $Li_3V_2(PO_4)_3$/C cathode material.

Acknowledgments

This work was supported by the National Natural Science Foundation of China (NSFC, Grant no. 20506024), State Key Development Program for Basic Research of China (Grant no. 2007CB216409), Zhejiang Provincial Natural Science Foundation of China (Grant no. LQ12B01003), Zhejiang University of Technology start-up fund (Grant no.101009529), Natural Science Foundation of China (21173190), the International Science and Technology Cooperation Program of China (2012DFG42100) and the Doctoral Program of Higher Education of China (2011010113003).

References

[1] A. Kuwahara, S. Suzuki, M. Miyayama, High-rate properties of $LiFePO_4$/carbon composites as cathode materials for lithium-ion batteries, Ceramics International 34 (4) (2008) 863–866.

[2] T. Yuan, R. Cai, K. Wang, R. Ran, S. Liu, Z. Shao, Combustion synthesis of high-performance $Li_4Ti_5O_{12}$ for secondary Li-ion battery, Ceramics International 35 (5) (2009) 1757–1768.

[3] S. Bao, Y. Liang, W. Zhou, B. Liu, H. Li, Synthesis and electrochemical properteis of $LiMn_2O_4$ by microwave assisted sol–gel method, Materials Letters 59 (2005) 3761–3765.

[4] T. Honma, K. Nagamine, T. Komatsu, Fabrication of olivine-type $LiMn_xFe_{1-x}PO_4$ crystals via the glass–ceramic route and their lithium ion battery performance, Ceramics International 36 (3) (2010) 1137–1141.
[5] S. Kikkawa, Titanium disulphide thin film prepared by plasma-CVD for lithium secondary battery, Ceramics International 23 (1) (1997) 7–11.
[6] B.-H. Kim, J.-H. Kim, I.-H. Kwon, M.-Y. Song, Electrochemical properties of $LiNiO_2$ cathode material synthesized by the emulsion method, Ceramics International 33 (5) (2007) 837–841.
[7] A. Yamada, S.C. Chung, Crystal chemistry of the olivine-type $Li(Mn_yFe_{1-y})PO_4$ and $(Mn_yFe_{1-y})PO_4$ as possible 4 V cathode materials for lithium batteries, Journal of the Electrochemical Society 148 (2001) A960–A967.
[8] W.L. Liu, J.P. Tu, Y.Q. Qiao, J.P. Zhou, S.J. Shi, X.L. Wang, C.D. Gu, Optimized performances of core-shell structured $LiFePO_4$/C nanocomposite, Journal of Power Sources 196 (2011) 7728–7735.
[9] M. Minakshi, P. Singh, D. Appadoo, D.E. Martin, Synthesis and characterization of olivine $LiNiPO_4$ for aqueous rechargeable battery, Electrochimica Acta 56 (2011) 4356–4360.
[10] Y.Q. Qiao, X.L. Wang, Y.J. Mai, J.Y. Xiang, D. Zhang, C.D. Gu, J.P. Tu, Synthesis of plate-like $Li_3V_2(PO_4)_{(3)}$/C as a cathode material for Li-ion batteries, Journal of Power Sources 196 (2011) 8706–8709.
[11] T. Jiang, Y.J. Wei, W.C. Pan, Z. Li, X. Ming, G. Chen, C.Z. Wang, Preparation and electrochemical studies of $Li_3V_2(PO_4)_{(3)}$/Cu composite cathode material for lithium ion batteries, Journal of Alloys and Compounds 488 (2009) L26–L29.
[12] M.M. Ren, Z. Zhou, Y.Z. Li, X.P. Gao, J. Yan, Preparation and electrochemical studies of Fe-doped $Li_3V_2(PO_4)_{(3)}$ cathode materials for lithium-ion batteries, Journal of Power Sources 162 (2006) 1357–1362.
[13] M.Y. Saidi, J. Barker, H. Huang, J.L. Swoyer, G. Adamson, Performance characteristics of lithium vanadium phosphate as a cathode material for lithium-ion batteries, Journal of Power Sources 119 (2003) 266–272.
[14] S.C. Yin, H. Grondey, P. Strobel, M. Anne, L.F. Nazar, Electrochemical property: structure relationships in monoclinic $Li_{3-y}V_2(PO_4)_{(3)}$, Journal of the American Chemical Society 125 (2003) 10402–10411.
[15] X.H. Rui, C. Li, C.H. Chen, Synthesis and characterization of carbon-coated $Li_3V_2(PO_4)_{(3)}$ cathode materials with different carbon sources, Electrochimica Acta 54 (2009) 3374–3380.
[16] Y.N. Ko, H.Y. Koo, J.H. Kim, J.H. Yi, Y.C. Kang, J.H. Lee, Characteristics of $Li_3V_2(PO_4)_{(3)}$/C powders prepared by ultrasonic spray pyrolysis, Journal of Power Sources 196 (2011) 6682–6687.
[17] J.W. Wang, X.F. Zhang, J. Liu, G.L. Yang, Y.C. Ge, Z.J. Yu, R.S. Wang, X.M. Pan, Long-term cyclability and high-rate capability of $Li_3V_2(PO_4)_{(3)}$/C cathode material using PVA as carbon source, Electrochimica Acta 55 (2010) 6879–6884.
[18] Q. Kuang, Y.M. Zhao, X.N. An, J.M. Liu, Y.Z. Dong, L. Chen, Synthesis and electrochemical properties of Co-doped $Li_3V_2(PO_4)_{(3)}$ cathode materials for lithium-ion batteries, Electrochimica Acta 55 (2010) 1575–1581.
[19] J.S. Huang, L. Yang, K.Y. Liu, Y.F. Tang, Synthesis and characterization of $Li_3V_{(2-2x/3)}Mg_x(PO_4)_{(3)}$/C cathode material for lithium-ion batteries, Journal of Power Sources 195 (2010) 5013–5018.
[20] J. Barker, R.K.B. Gover, P. Burns, A.J. Bryan, A lithium-ion cell based on $Li_{4/3}Ti_{5/3}O_4$ and $LiVPO_4F$, Electrochemical and Solid State Letters 10 (2007) A130–A133.
[21] Y.G. Mateyshina, N.F. Uvarov, Electrochemical behavior of $Li_{(3-x)}M'_{(x)}V_{(2-y)}M''_{(y)}(PO(4))_{(3)}$ (M ‘=K, M ‘‘=Sc, Mg plus Ti)/C composite cathode material for lithium-ion batteries, Journal of Power Sources 196 (2011) 1494–1497.
[22] Y.H. Chen, Y.M. Zhao, X.N. An, J.M. Liu, Y.Z. Dong, L. Chen, Preparation and electrochemical performance studies on Cr-doped $Li_3V_2(PO_4)_{(3)}$ as cathode materials for lithium-ion batteries, Electrochimica Acta 54 (2009) 5844–5850.
[23] C.S. Sun, Y. Zhang, X.J. Zhang, Z. Zhou, Structural and electrochemical properties of $LiFePO_4$/C, Journal of Power Sources 195 (2010) 3680–3683.
[24] S. Bao, Y. Liang, W. Zhou, B. He, H. Li, Synthesis and electrochemical properteis of $LiAl_{0.1}Mn_{0.9}O_4$ by microwave-assistted sol–gel method, Journal of Power Sources 154 (2006) 239–245.
[25] S.R. Vallance, D.M. Round, C. Ritter, E.J. Cussen, S. Kingman, D.H. Gregory, Ultra-rapid microwave synthesis of superconducting refractory carbides, Advanced Materials 21 (2009) 4502–4504.
[26] W.R. Liu, S.H. Wu, H.S. Sheu, Preparation of spinel $Li_{(1.06)}Mn_{(2)}O_{(4-z)}Cl_{(z)}$ cathode materials by the citrate gel method, Journal of Power Sources 146 (2005) 232–236.
[27] C.S. Dai, Z.Y. Chen, H.Z. Jin, X.G. Hu, Synthesis and performance of $Li_3(V_{1-x}Mg_x)_{(2)}(PO_4)_{(3)}$ cathode materials, Journal of Power Sources 195 (2010) 5775–5779.
[28] J.W. Wang, J. Liu, G.L. Yang, X.F. Zhang, X.D. Yan, X.M. Pan, R.S. Wang, Electrochemical performance of $Li_3V_2(PO_4)_{(3)}$/C cathode material using a novel carbon source, Electrochimica Acta 54 (2009) 6451–6454.
[29] Y.Q. Qiao, J.P. Tu, X.L. Wang, D. Zhang, J.Y. Xiang, Y.J. Mai, C.D. Gu, Synthesis and improved electrochemical performances of porous $Li_3V_2(PO_4)_{(3)}$/C spheres as cathode material for lithium-ion batteries, Journal of Power Sources 196 (2011) 7715–7720.
[30] J.H. Yao, S.S. Wei, P.J. Zhang, C.Q. Shen, K.-F. Aguey-Zinsou, L.B. Wang, Synthesis and properties of $Li_3V_{2-x}Ce_x(PO_4)_3$/C cathode materials for Li-ion batteries, Journal of Alloys and Compounds 532 (2012) 49–54.
[31] J. Barker, M.Y. Saidi, J.L. Swoyer, A carbothermal reduction method for the preparation of electroactive materials for lithium ion applications, Journal of the Electrochemical Society 150 (2003) A684–A688.